

Opinion dynamics in a three-choice system

S. Gekle^{1,a}, L. Peliti^{2,b}, and S. Galam^{1,c}

¹ Centre de Recherche en Épistémologie Appliquée, CREA-École Polytechnique, CNRS UMR 7656, 1, rue Descartes, 75005 Paris, France

² Dipartimento di Scienze Fisiche and Unità INFN, Università “Federico II”, Complesso Monte S. Angelo, 80126 Napoli, Italy

Received 1st January 2005

Published online 13 July 2005 – © EDP Sciences, Società Italiana di Fisica, Springer-Verlag 2005

Abstract. We generalize Galam’s model of opinion spreading by introducing three competing choices. At each update, the population is randomly divided in groups of three agents, whose members adopt the opinion of the local majority. In the case of a tie, the local group adopts opinion A, B or C with probabilities α , β and $(1 - \alpha - \beta)$ respectively. We derive the associated phase diagrams and dynamics by both analytical means and simulations. Polarization is always reached within very short time scales. We point out situations in which an initially very small minority opinion can invade the whole system.

PACS. 87.23.Ge Dynamics of social systems – 05.65.+b Self-organized systems

1 Introduction

In recent years, the field of Sociophysics [1,2] has drawn a growing interest from physicists, mostly theoreticians, with the study of opinion dynamics as one of the most active subjects [3–11]. A simple model of opinion spreading with two choices was introduced some time ago by one of the authors [12]. In this model the system will eventually reach a homogeneous state called polarization by repeated debates. In this model, at each time step, the population is divided at random into groups of size m , and each group adopts the opinion of the local majority. This dynamics is called *randomly localized* with a *local majority* rule. With two choices, if m is odd, there are no ties and even a slight deviation from a 50/50 initial distribution eventually leads to the polarization of the majority opinion [12,13].

Here we investigate the richer dynamics provided by an $m = 3$ system with *three* possible choices, which we shall label by A, B, and C. This leads to the possibility of ties, when each member of the group has a different opinion [14,15]. We introduce the probabilities α , β and $(1 - \alpha - \beta)$ of resolving the tie in favor of A, B and C respectively. An alternative proposal for the discussion dynamics has been considered in reference [16], where quantities analogous to α and β allow for a contextual interpretation. The quantum nature of these models could reflect

more precisely the “reduction process” by which a discussant takes up an opinion.

In our model we find that polarization is always reached in a short time, and that it is possible to summarize the behavior of the system (for given values of α and β) by associating to each initial opinion distribution the value of the opinion which eventually prevails. We can thus draw phase diagrams, exhibit phase separation lines and fixed points. In particular it is found that in some circumstances an initially very small minority opinion can invade the whole system. While the phase boundaries are sharp in the limit of large populations, simulations show that they become blurred when the population is small, since starting from the same initial condition may lead to the polarization of different opinions. The polarization time also exhibits larger fluctuations, always remaining very small.

In Section 2, after a brief review of the standard Galam model with two choices [12], we define the model with three choices and we derive the basic evolution equations. The fixed points and flows of these equations are discussed in Section 3. These analytical predictions are compared against numerical simulations in Section 4. Section 5 contains some concluding remarks and proposes some research possibilities.

2 The model

We first describe the randomly localized dynamics with local majority rule for the standard Galam model [12,13] with two choices, and we then introduce our present model with three choices.

^a e-mail: sgekle@gmx.net

^b Associated to INFN, Sezione di Napoli
e-mail: peliti@na.infn.it

^c e-mail: galam@ccr.jussieu.fr

We consider a population of N agents, each of which can have opinion A or opinion B. At each time step, the whole population is divided into groups of size m , so that each agent belongs to one and only one group. Discussions take place, and at the end of the discussion all the members of the group adopt the opinion of the local majority. The process is iterated until a stable situation is reached.

With $m = 3$, ties are ruled out and we can write outright the evolution equation for the fraction p_A of agents with opinion A [13]:

$$p_A(t+1) = p_A^3(t) + 3p_A^2(t)(1 - p_A(t)). \quad (1)$$

This evolution exhibits the two stable fixed points at $p_A = 0$, $p_A = 1$, and an unstable fixed point at $p_A = \frac{1}{2}$, which defines the phase boundary. This means that an initial condition slightly different from 50/50 will always lead to a complete polarization of the system, since the flow is drawn towards one of the stable fixed points.

When there are three choices, A, B and C, there is the possibility of a tie in which each agent has a different opinion. We assume that the tie is always resolved in favor of one of the opinions, and we introduce the probabilities α , β and $\gamma = 1 - \alpha - \beta$ that the winning opinion is A, B, or C respectively. Thus, e.g., the three members of a group will come out with opinion A if one of these cases applies:

1. They all already have opinion A, which happens with probability p_A^3 ;
2. Two of them have opinion A, which happens with probability $3p_A^2(1 - p_A)$;
3. There is a tie resolved in favor of A, which happens with probability $6\alpha p_A p_B(1 - p_A - p_B)$.

A similar analysis can be made for p_B . We consider the large population limit, in which sampling fluctuations can be neglected. We thus obtain the evolution equations for the fractions p_A , p_B :

$$p_A(t+1) = p_A^3(t) + 3p_A^2(t)(1 - p_A(t)) + 6\alpha p_A(t)p_B(t)(1 - p_A(t) - p_B(t)); \quad (2)$$

$$p_B(t+1) = p_B^3(t) + 3p_B^2(t)(1 - p_B(t)) + 6\beta p_A(t)p_B(t)(1 - p_A(t) - p_B(t)). \quad (3)$$

The state of the system can be conveniently represented by a point in an equilateral triangle. Let \mathbf{A} , \mathbf{B} and \mathbf{C} be the vertices of such a triangle, then the state defined by the probabilities p_A , p_B and $p_C = 1 - p_A - p_B$ is represented by the point

$$\mathbf{p} = p_A \mathbf{A} + p_B \mathbf{B} + p_C \mathbf{C} = \mathbf{C} + p_A \overline{\mathbf{CA}} + p_B \overline{\mathbf{CB}}, \quad (4)$$

where $\overline{\mathbf{CA}}$ and $\overline{\mathbf{CB}}$ are the vectors leading from \mathbf{C} to \mathbf{A} and \mathbf{B} respectively. The vertices of the triangle represent the polarized states. Inspection of equations (2, 3) (and common sense) shows that these states are fixed and stable. Each vertex thus commands a nonempty attraction basin. Indeed, one can see that if, e.g., $\frac{1}{2} < p_A(t) < 1$, one has $p_A(t+1) > p_A(t)$. Thus the attraction basin of \mathbf{A} contains at least the region $p_A > \frac{1}{2}$.

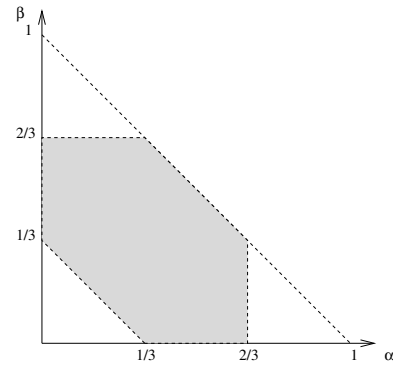


Fig. 1. The region in the (α, β) plane in which the inner fixed point G appears is dashed.

3 Fixed points and flow diagrams

Equations (2, 3) exhibit the following fixed points:

1. The trivial fixed points A, B and C, corresponding to the polarized states;
2. Since, when one of the three fractions p_A , p_B or p_C vanishes, the evolution equations reduce to the one describing the two-choice Galam model (Eq. (1)), there are the corresponding fixed points D ($p_A = \frac{1}{2}$, $p_B = \frac{1}{2}$), E ($p_B = \frac{1}{2}$, $p_C = \frac{1}{2}$), and F ($p_C = \frac{1}{2}$, $p_A = \frac{1}{2}$) which lie on the triangle sides.
3. Moreover a seventh fixed point G, in which all three fractions are nonzero, may appear in the DEF triangle. For this point to appear, it is necessary that none of the probabilities α , β and $\gamma = 1 - \alpha - \beta$ is larger than $\frac{2}{3}$. Thus the region in the (α, β) plane in which this G point appears is the one dashed in Figure 1.

The stability of the fixed points can as usual be discussed by linearizing the evolution equations around them. If we denote by J the Jacobian matrix of the transformations (2, 3), a fixed point is stable if all the eigenvalues of J are smaller than 1 in absolute value. One can easily check that:

1. The three trivial fixed points A, B and C have all eigenvalues equal to 0;
2. The three side points D, E and F, have one eigenvalue equal to $\frac{3}{2}$, corresponding to the eigenvector lying along the side of the triangle, whereas the other one is given by

$$\frac{3}{2}(1 - \alpha - \beta) \text{ for D, } \frac{3}{2}\alpha \text{ for E, and } \frac{3}{2}\beta \text{ for F.} \quad (5)$$

- We see that the direction towards the interior of the triangle becomes unstable if the probability parameter associated with the opposite vertex is larger than $\frac{2}{3}$. In this situation, the inner fixed point does not exist.
3. The inner fixed point, if it exists, has both eigenvalues larger than 1 in modulus.

The basic structure of the flow is thus represented in Figure 2. The first applies to the case in which there is the inner fixed point, G, (Case I) and the other to the case in

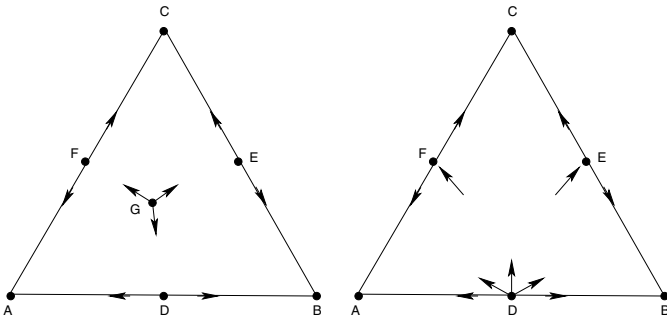


Fig. 2. Fixed points and basic structure of the flow. Left: Case I, in which (α, β) lies inside of the dashed region in Figure 1. Right: Case II, in which (α, β) lies outside that region. In the case shown, $\gamma = 1 - \alpha - \beta > \frac{2}{3}$.

which it does not exist (Case II). It is clear from this figure that, in Case I, the attraction basins of the stable fixed points meet two by two at the fixed points D, E and F, and all three in the inner point G. In Case II, on the other hand, the attraction basin of the point corresponding to the largest favorable probability (α for A, etc.) will separate the basins of the other fixed points at the side fixed point situated midway between the two.

The phase boundaries can be conveniently located by iterating the inverse of equations (2, 3), starting close to the side fixed points D, E, or F. The iterations converge to the inner fixed point G, if it exists, or to the other relevant side fixed point. As an example, we show in Figure 3 the phase diagram obtained for $\alpha = \beta = \frac{1}{4}$ and $\frac{1}{6}$ respectively. It is clear that the attraction basins of the side fixed points reduce to stretches of the phase boundaries: the one connecting each point to G, in Case I, or to the unstable side fixed point (like D in Fig. 3, right), in Case II. In Figures 4 and 5 we show respectively the flow and the phase diagrams for $\alpha = 1/2, \beta = 1/3$ (Case I) and for $\alpha = 2/9, \beta = 1/9$. We can conclude that in Case II, close to the unstable side fixed point, there is the possibility that the “preferred” opinion (the one with the largest probability of resolving a tie) can invade the system even if it is initially supported by a very small minority. The width of the sector in the $\mathbf{p} = (p_A, p_B)$ plane where this can happen rapidly vanishes as \mathbf{p} approaches the side of the triangle, since the two boundary lines are tangent to each other (unless $\alpha = \beta = 0$). The sector, however, opens up more and more rapidly as the third opinion becomes more and more preferred.

If one of the three probabilities (e.g., β) vanishes, the straight line $p_B = \frac{1}{2}$, connecting the side fixed points D and E on either side of the corresponding vertex B, is conserved by the flow and defines the boundary of the attraction basin for it. This means that the “unpreferred” opinion can invade only if it is initially shared by a majority. For $\alpha < \frac{1}{3}$ the fixed point E is stable along this line. For $\frac{1}{3} < \alpha < \frac{2}{3}$ the inner fixed point G appears on the line, and both side fixed points D and E are partially stable. Finally, if $\alpha > \frac{2}{3}$, the fixed point D becomes partially stable, while E becomes totally unstable. The different cases are represented in Figure 6.

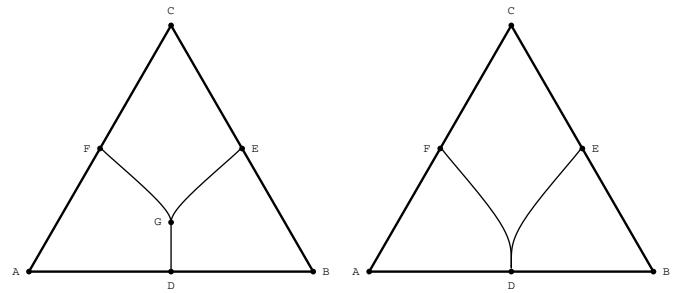


Fig. 3. Phase diagrams for the dynamics: Left: $\alpha = \beta = \frac{1}{4}$ (Case I). Right: $\alpha = \beta = \frac{1}{6}$ (Case II).

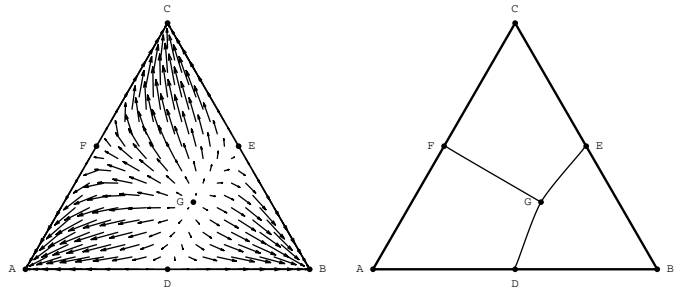


Fig. 4. Flow, fixed points and attraction basins for $\alpha = 4/9, \beta = 1/9$ (Case I). Left: Flow and fixed points. Right: Boundaries of the attraction basin.

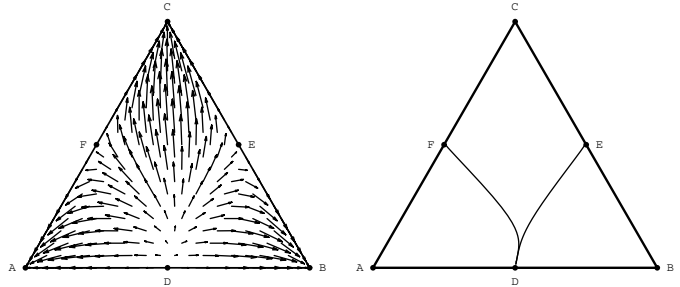


Fig. 5. Flow, fixed points and attraction basins for $\alpha = 2/9, \beta = 1/9$ (Case II). Left: Flow and fixed points. Right: Boundaries of the attraction basin.

4 Simulations

4.1 Phase diagram

We now consider the behavior of systems with finite values of N . Equations (2, 3) provide a good description of its behavior, provided one decrees that complete polarization has taken place whenever

$$p_i < \frac{1}{N}, \quad i \in \{A, B, C\}. \quad (6)$$

In this case, indeed, every single agent supports the winning opinion. For N large enough, the attraction basins we have identified on the basis of the iteration equations hold with practical certainty, except very close to the boundaries. When N gets smaller, one can see some uncertainty building up along the boundaries, as shown in Figure 7. Here we assign a color to each of the vertices of the triangle (black for A, light grey for B, and dark grey for C)

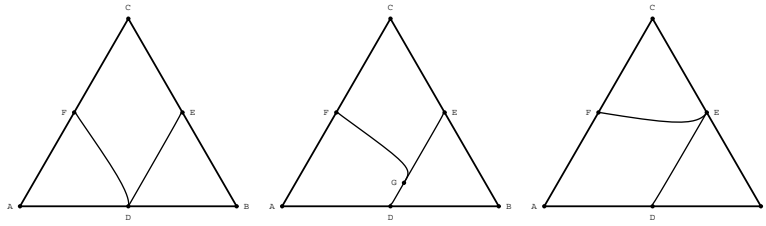


Fig. 6. Phase diagrams with $\beta = 0$. The straight line DE ($p_B = \frac{1}{2}$) is conserved by the flow. Left: $\alpha = \frac{1}{10}$. Center: $\alpha = \frac{5}{12}$; Right: $\alpha = \frac{5}{6}$.

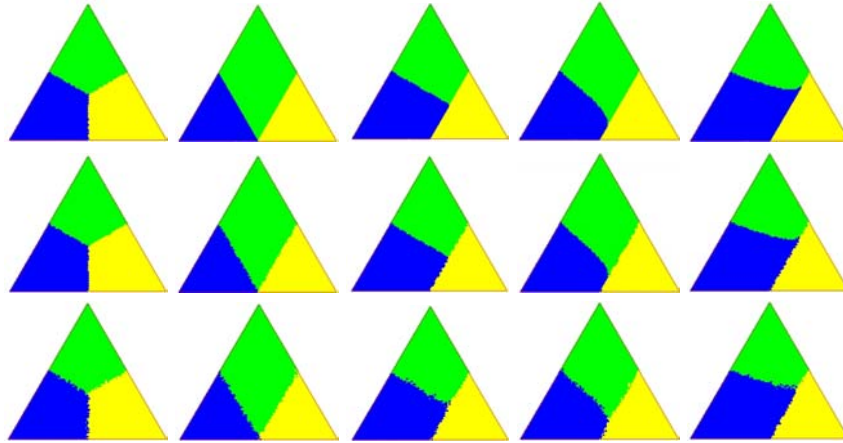


Fig. 7. Simulated phase diagrams for (from left to right) $\alpha = \beta = \frac{1}{3}$; $\alpha = \beta = 0$; $\alpha = \frac{1}{2}$ and $\beta = 0$; $\alpha = \frac{1}{3}$ and $\beta = 0$; $\alpha = \frac{2}{3}$ and $\beta = 0$. From top to bottom system sizes of $N = 10^4$, $N = 2500$ and $N = 100$. The color of a point corresponds to the vertex reached most often in 50 runs, starting from that initial condition. One can see how the boundary lines become blurred for small systems.

and we assign to each of the initial conditions (a point (p_A^0, p_B^0) in the triangle) the color of the vertex reached most often in 50 trials. The diagram is evaluated on approximately 5000 different initial conditions with different values of N : $N = 10^4$, $N = 2500$, and $N = 100$. It is clear that while the overall shape of the phase diagram remains unchanged, the phase boundaries become more and more blurred as N decreases.

To get a more precise measure of the difference between the results of simulations and the predictions of the deterministic equations, we compared the phase diagrams one by one for all 5100 initial distributions and counted the percentage of mismatches. Results are shown in Table 1. One can see how the quality of agreement diminishes with smaller system sizes, but can be improved again by increasing the number of runs over which the statistical average is taken. This improvement only works up to a certain level, though, the error margins for 5000 runs in a system with $N = 100$ stay almost exactly the same as for 1000 runs and are therefore not shown here. As one can see in Figure 7, the mismatches occur only around the phase separation lines. As soon as the initial distribution is set a small distance apart from these lines, the percentage of mismatch goes towards 0. As the error even for small systems with $N = 100$ and only 50 runs is maximal at 2.4%, we conclude that the deterministic equations (2, 3) work very well for phase diagrams down to this size.

4.2 Polarization time

It is also interesting to discuss the polarization time T_p , i.e., the number of discussion cycles needed to reach complete polarization. It depends on the initial condition as well as α and β . We list in Table 2 polarization times for a few interesting configurations. In Figure 8 the polarization times are displayed as a function of the initial condition over the whole triangle. One can see that the polarization time becomes longer as the initial distributions approaches the phase boundaries. The scaling of T_p with system size N , using the deterministic evolution equations, is shown in Figure 9 for two configurations, one with an initial distribution close to the triple point G with $\alpha = \beta = 0$ starting from $p_A = 0.51$ and $p_B = 0.49$, the other far from the triple point with $\alpha = \beta = \frac{1}{3}$ starting from $p_A = p_B = 0.1$. One sees that, even if N varies from 25 to 10^8 , T_p remains virtually constant, varying only between 11 and 14 in the first and between 2 and 5 in the second case.

The scaling of the simulated polarization time for the same configurations as above is shown in Figure 10. The picture now looks quite different than for the phase diagrams. Regarding T_p only for systems with about 1000 agents the agreement is still acceptable, although the error bars are already quite large. Overall the agreement for the system starting far from the triple point is much better than for the system starting close to it.

Table 1. Percentage of mismatching points between probability calculations and simulations for different system sizes.

	$N = 10^4$ (50 runs)	$N = 2500$ (50 runs)	$N = 100$ (50 runs)	$N = 100$ (100 runs)	$N = 100$ (1000 runs)
$\alpha = \frac{1}{3}, \beta = \frac{1}{3}$	0.7%	1.0%	1.8%	1.5%	1.0%
$\alpha = 0, \beta = 0$	0.1%	2.0%	2.4%	2.1%	2.1%
$\alpha = \frac{1}{2}, \beta = 0$	0.5%	1.5%	2.2%	1.9%	1.6%
$\alpha = \frac{1}{3}, \beta = 0$	0.1%	1.1%	2.0%	1.7%	1.3%
$\alpha = \frac{2}{3}, \beta = 0$	0.1%	1.2%	1.8%	1.6%	1.4%

Table 2. Polarization time T_p for a few interesting configurations. Results obtained by the evolution equations (2, 3) and by simulations for a system of $N = 10^4$. Simulated results averaged over 100 runs.

α	β	p_A	p_B	winner	time T_p (probabilities)	time T_p (simulated)
0	0	1	0	A	0	0 ± 0
0	0	0.51	0.49	A	13	13.1 ± 1.4
0	0	0.49	0.49	C	13	13.8 ± 1.1
0	0	0.30	0.30	C	5	5.4 ± 0.5
0	0	0.1	0.1	C	3	3.1 ± 0.3
1/3	1/3	0.1	0.1	C	4	4.0 ± 0.3
1/2	0	0.1	0.1	C	4	4.0 ± 0.2
1/2	0	0.3	0.51	B	13	13.2 ± 1.4

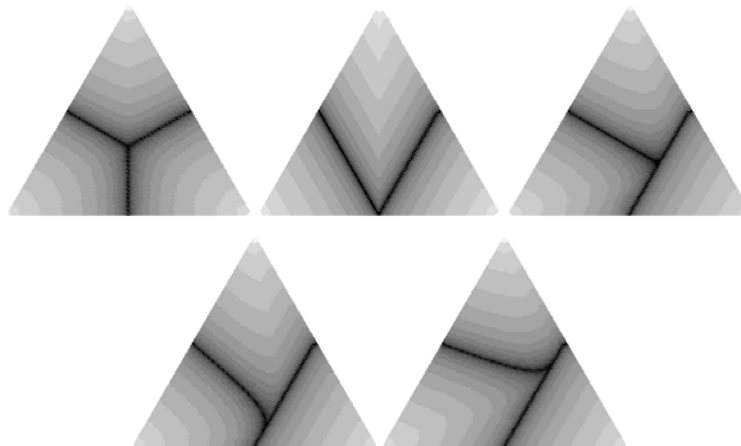


Fig. 8. Polarization time T_p in a system with $N = 10^4$ for different parameters obtained by the deterministic evolution equations (2, 3). Darker colors mean longer time. Note the peaks around the phase boundaries. Above: left: $\alpha = \beta = \frac{1}{3}$; center: $\alpha = \beta = 0$; right: $\alpha = \frac{1}{2}, \beta = 0$. Below: left: $\alpha = \frac{1}{3}, \beta = 0$; right: $\alpha = \frac{2}{3}, \beta = 0$.

Looking at the relative error shown in Figure 11, one must suggest that for small systems with $N < 1000$ a prediction of the polarization time via the evolution equations (2, 3) is unreliable. However, predictions about the winning opinion remain fairly reliable as described in the previous section.

5 Concluding remarks

In this paper we presented an extension of Galam’s model for a two-choice system [13] to a system in which each agent can choose between three possible opinions. All research has been done for discussion groups of size 3 and in a randomly-localized model. To resolve ties, two new parameters α and β measuring “argument strength” were

introduced. Opinion distributions could be conveniently visualized in an equilateral triangle.

We showed that, independent of the parameter values, the system will almost always reach a complete polarization after a small number of discussion cycles. These polarization times are virtually independent of system size. We have drawn the phase diagrams, associating to each initial condition (p_A^0, p_B^0) the opinion (A, B, or C) which eventually wins. Finally, a number of simulations has been conducted to show that the deterministic evolution equations used to obtain the above results are reliable down to systems with approximately 100 agents, as far as the phase diagram is concerned, and to $N \simeq 1000$ for the polarization times.

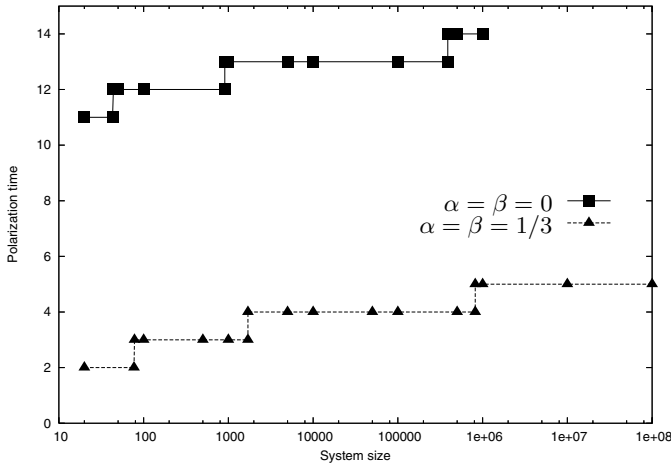


Fig. 9. Polarization times T_p obtained by iteration of equations (2, 3) for different system sizes. The system starts from $p_A = 0.51$, $p_B = 0.49$ for the case $\alpha = \beta = 0$ (squares) and from $p_A = 0.1$, $p_B = 0.1$ for $\alpha = \beta = 1/3$ (triangles). The same convention applies to Figures 10 and 11. The system starting far from the triple point G (lower curve) converges a lot faster on a polarization. Even over a wide range of system sizes T_p remains virtually constant.

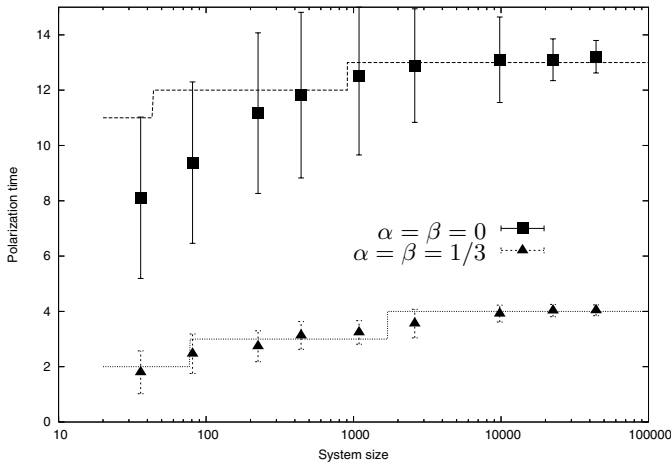


Fig. 10. Polarization times T_p obtained through simulations for different system sizes. As expected, the error bars become smaller with increasing system size. Overall, error bars for the system starting far from the triple point G are much smaller than for the other system. Results averaged over 100 runs.

Similar phase diagrams are obtained with a serial update dynamics, in which, at each microscopic time step, three different agents are picked up at random and their opinions updated according to the local majority rule described above. One counts a time step when each individual has taken part to three discussions on average. The polarization times with this dynamics are longer. Indeed, while in the parallel dynamics discussed so far the approach to the stable fixed points is ultrafast (the deviation gets squared at each time step) it is only exponential in

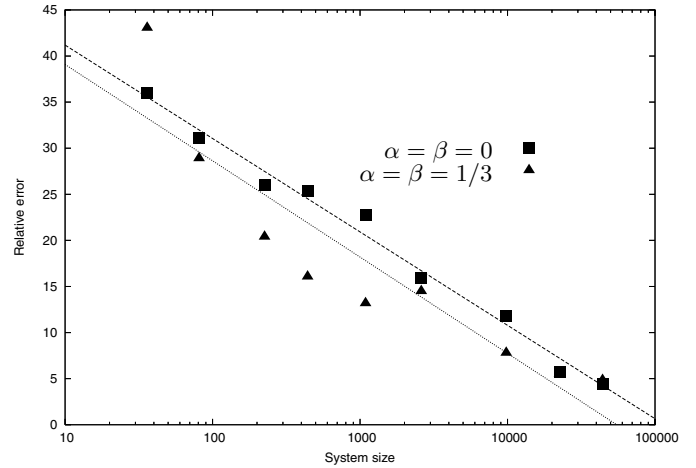


Fig. 11. Relative error of the simulated polarization time T_p . For systems with $N < 1000$ the error becomes very large and predictions seem unreliable.

the serial update dynamics. Thus

$$T_p \sim \begin{cases} \sqrt{\ln N}, & \text{with parallel dynamics;} \\ \ln N, & \text{with serial dynamics.} \end{cases} \quad (7)$$

Our results show that dealing with three opinions is much more complex than with two. From the complexity of the various flows, it is seen that initial conditions are not enough to predict any outcomes since the values of the parameters α and β are instrumental to determine the highly nonlinear road to success or failure in the rather quick competition in the opinion forming process. What appears as a successful strategy for one opinion in the first steps may turn out to be a total disaster at the end. At this stage of our investigation the following clues can be outlined.

1. It seems that we have here some hint on why the various attempts to create a “third way” in democratic countries have always failed. Starting from an A-B two-party situation two possibilities exist for the creation of a third one C. Either it is created on its own against A and B or it is “helped” by one of the two big forces, say A. In the first case we have $\alpha = \beta = \frac{1}{3}$ making C much further from the boundaries since by its nature it is a new comer. Therefore it will rather quickly disappear. In the second case we have $\alpha = \beta = 0$ since at a tie, A goes for C. In this case C will start growing slowly at the expense of both B and A. To stop it from spreading all over the unique solution is to have A and B to make a coalition against C with $\alpha = \beta = \frac{1}{2}$.
2. Focusing on the polarization effect with one opinion spreading in two opinion competitions, it seems that the best strategy is not to reinforce its own side but instead to create a third opinion which cooperates with either one of the others. It makes the new very minority opinion to eventually win the competition.

The above ideas are of course qualitative and need to be deepened. This paper is just a beginning outlining some

basic features of three-opinion systems. There is much room for further research, as for example the introduction of a geographical distribution and the influence of neighborhood relations [5]. Another interesting topic would be the behavior of discussion groups with more than three members [14]. To introduce some dependence of the parameters α and β on the values of the respective support for A and B would be also of a great interest.

We would like to thank the COST organization for a scholarship to support S. Gekle's stay in Paris, where this paper was written. S. Galam is grateful to INFM for supporting his trip to Naples, where this collaboration was started.

References

1. S. Galam, Y. Gefen, Y. Shapir, *Math. J. Sociology* **9**, 1 (1982)
2. S. Galam, *Physica A* **336**, 49 (2004)
3. M.C. Gonzalez, A.O. Sousa, H.J. Herrmann, to appear in *Int. J. Mod. Phys. C* **15** (2004)
4. F. Wu, B.A. Huberman, [arXiv: cond-mat/0407252](https://arxiv.org/abs/cond-mat/0407252)
5. C.J. Tessone, R. Toral, P. Amengual, H.S. Wio, M. San Miguel, *Eur. Phys. J. B* **39**, 535 (2004)
6. F. Slanina, H. Lavicka, *Eur. Phys. J. B* **35**, 279 (2003)
7. D. Stauffer, *Journal of Artificial Societies and Social Simulations* **5**, No. 1 paper 4, and *AIP Conference Proceedings* **690**, 147 (2003)
8. F. Schweitzer, J. Zimmermann, H. Mühlenbein, *Physica A* **303**, 189 (2002)
9. G. Deffuant, D. Neau, F. Amblard, G. Weisbuch, *Adv. Complex Systems* **3**, 87 (2001)
10. K. Sznajd-Weron, J. Sznajd, *Int. J. Mod. Phys. C* **11**, 1157 (2000)
11. S. Solomon, G. Weisbuch, L. de Arcangelis, N. Jan, D. Stauffer, *Physica A* **277**, 239 (2000)
12. S. Galam, *J. Math. Psychology* **30**, 426 (1986); S. Galam, *J. Stat. Phys.* **61**, 943 (1990)
13. S. Galam, *Eur. J. Phys. B* **25**, 403 (2002)
14. S. Galam, *Int. J. General Systems* **18**, 191 (1991)
15. S. Galam, *Physica A* **285**, 66 (2000)
16. D. Aerts, S. Aerts, *Foundations of Science* **1**, 85 (1995), reprinted in *Topics in the Foundation of Statistics*, edited by B. Van Fraassen (Kluwer, Dordrecht, 1997)